Structure and Activity of an Active Site Substitution of Ricin A Chain[†,‡]

Philip J. Day,[§] Stephen R. Ernst,[§] Arthur E. Frankel,[||] Arthur F. Monzingo,[§] John M. Pascal,[§] Maria C. Molina-Svinth,[§] and Jon D. Robertus*[,§]

Department of Chemistry and Biochemistry, University of Texas, Austin, Texas 78712, and Florida Hospital Cancer Center, 2501 North Orange Avenue, Suite 201, Orlando, Florida 32804

Received April 12, 1996; Revised Manuscript Received June 19, 1996[⊗]

ABSTRACT: The A chain of ricin (RTA) is an *N*-glycosidase which inactivates ribosomes by removing a single adenine base from a conserved region of rRNA. X-ray structures and site-directed mutagenesis revealed that Arg 180 interacts with the target adenine hydrogen bonding with N3. It may fully or partially protonate that atom as part of the hydrolysis mechanism. Arg 180 was previously converted to His (R180H) and shown to greatly reduce activity. Here R180H is shown to reduce overall activity 500-fold against *Artemia salina* ribosomes. A 2.2 Å crystal structure reveals the mutation causes a rearrangement of the active site cleft, with Tyr 80 moving to block access to the adenine recognition site. His 180 forms a strong aromatic interaction with Trp 211, Tyr 80, and Tyr 123. A complex is formed with 250 mM AMP. The nucleotide binds in the active site region, but in an apparently nonproductive orientation. His 180 cannot bond to N3 and is screened from the substrate analog by the intervening Tyr 80. It may be that natural polynucleotide substrates, using additional interactions, can displace Tyr 80 and effect a productive binding.

Ricin, a potent cytotoxin isolated from castor beans, is composed of two disulfide-linked subunits (reviewed in Olsnes and Pihl, 1982). The ricin B-chain (RTB) is a galactose binding lectin which promotes binding to cell surfaces and entry into the cell by receptor mediated endocytosis. Once inside the cell, the disulfide bond between RTB and the A-chain (RTA) is reduced and RTA enters the cytoplasm by translocation across an as yet unidentified internal membrane. RTA is homologous to an increasingly large family of plant-derived ribosome inactivating proteins (RIPs) which catalyze the removal of a specific adenine residue (A_{4324} in rat) from 28S ribosomal RNA, thus inhibiting protein synthesis (Endo & Tsurugi, 1988). Ricin is a type II RIP, having both A and B chains, and is extremely toxic to eukaryotic cells. Type I RIPs (e.g., trichosanthin, pokeweed antiviral protein), however, possess only an RTA-like A chain and thus do not readily bind to cells and are considerably less cytotoxic.

Sequence alignment of type I RIPs and the A chains of type II RIPs revealed considerable similarity and identified a number of highly conserved residues. The role of several of these residues has been investigated by site-directed mutagenesis (Schlossman *et al.*, 1989; Frankel *et al.*, 1990; Ready *et al.*, 1991; Kim & Robertus, 1992), and Glu 177 and Arg 180 (RTA numbering) have been identified as the critical catalytic residues. The structures of ricin, RTA, and ricin·substrate analog complexes have been solved by X-ray crystallography (Montfort *et al.*, 1987; Rutenber *et al.*, 1991; Katzin *et al.*, 1991; Monzingo & Robertus, 1992). These structures were consistent with mutagenesis results, showing that the substrate adenine binds between two conserved tyrosines, 80 and 123, and that a strong hydrogen bond forms between Arg 180 and the N3 of the adenine. Glu 177 is positioned near the substrate ribose, but its exact role is less clear since the analog complexes may be in a lower energy configuration than the natural rRNA substrate (Monzingo & Robertus, 1992). More recently, the structure of an alternate crystal form of RTA has been refined to 1.8 Å resolution (Weston *et al.*, 1994) and the structure of α-momorcharin, an RTA homologue, has been solved (Ren *et al.*, 1994). On the basis of these structures, several variations on the RTA have been proposed in which the primary players are the same but their proposed roles differ. The principal differences in the mechanisms are (1) which residue activates the attacking water molecule, either Glu 177 or Arg 180; and (2) whether N3 of the substrate adenine is fully or partially protonated by Arg 180.

Arg 180 of RTA has been shown to play a crucial role in catalysis. Replacement of arginine by glutamine (R180Q) increases IC_{50} (the dose inhibiting 50% of activity) for *Artemia salinas* ribosomes by at least 250-fold. More sophisticated initial rate kinetics show a decrease in k_{cat} of more than 3 orders of magnitude (Kim & Robertus, 1991). A lysine at position 180 (R180K) shows only a 3-fold decrease in activity compared with wild-type, suggesting that it is the ionizable charged group on residue 180 that is critical (Frankel *et al.*, 1990).

Uracil−DNA glycosylase catalyses a similar reaction to that of RTA; the differences are that the base hydrolyzed is a misincorporated uracil and the substrate is DNA rather than RNA. The proposed enzymatic mechanisms are very similar, and the recent structure of uracil−DNA glycosylase revealed that the residue responsible for protonation of the leaving group, Arg 180 of RTA, is replaced by a histidine residue (Savva *et al.*, 1995). The other catalytically important

[†] This work was supported by Grants GM 30048 and GM35989 from the National Institutes of Health and by grants from the Foundation for Research and the Welch Foundation.

[‡] Coordinates have been deposited in the Brookhaven Protein Data Bank with entry numbers 1OBS and 1OBT.

* Corresponding author. Telephone: (512) 471-3175; Email: jrobertus@mail.utexas.edu.

[§] University of Texas.

[||] Florida Hospital Cancer Center.

[⊗] Abstract published in *Advance ACS Abstracts,* August 1, 1996.

S0006-2960(96)00880-X CCC: $12.00

residue, Glu 177, is replaced by Asp and is proposed to activate an attacking water molecule. Substitution of His 268 (with Leu) and Asp 145 (with Asn) of uracil−DNA glycosylase results in 300- and 2500-fold decreases in activity, respectively (Mol *et al.*, 1995).

In addition to mutation of Arg 180 to Gln and Lys, the site has also been converted to histidine (R180H) with at least a 1000-fold loss in activity (Frankel *et al.*, 1990). The relative inactivity of histidine compared to lysine was attributed to the reduced length of the side chain and hence inability to hydrogen bond to N3 of the adenine leaving group. Most enzymes enhance catalytic rates over uncatalyzed reactions by 10^{12}, and so although the R180H enzyme is reduced in activity compared to the wild-type and has an alteration at a critical catalytic residue, it is still a very good catalyst. This paper analyzes the activity and structure of the R180H protein, and a complex with AMP, to understand its catalytic effectiveness.

EXPERIMENTAL PROCEDURES

Expression and Purification of Recombinant RTA. Small (50 mL) cultures of *Escherichia coli* JM101 harboring plasmid pUTA (Ready *et al.*, 1991) or pUTA:R180H were grown overnight at 37 °C, then used to inoculate 500 mL of 2YT media, and grown for 2 h at 30 °C. Expression of RTA was induced by addition of 50 mL 0.5 M isopropyl 1-thio-β-D-galactoside (IPTG) and incubation for 4 h at 30 °C. Cells were harvested by centrifugation, resuspended in 30 mL of 5 mM sodium phosphate (pH 6.5), and broken with a French pressure cell. Following centrifugation to remove cell debris, the supernatant was loaded onto a 100 mL carboxymethyl-Sepharose (Pharmacia) column equilibrated in the same buffer. Unbound protein was washed from the column with 1500 mL of buffer followed by 200 mL of buffer containing 100 mM sodium chloride. RTA was eluted with a linear 500 mL 0.1−0.3 M sodium chloride gradient. Peak RTA containing fractions were pooled and stored at 4 °C at ∼1 mg/mL. Typical yields were 40−50 mg of RTA/L of media for wild-type RTA and 10−20 mg/L for RTA R180H.

Construction of RTA Y80F, R180H Double Mutant. Plasmids pUTA:R180H (Frankel *et al.*, 1990; Kim and Robertus, unpublished results) and pUTA:Y80F (Ready *et al.*, 1991) were digested with *Cla*I and *Bam*HI and ligated together at 15 °C for 18 h. Following transformation into *E. coli* JM101, isolated recombinant plasmids were screened by restriction analysis. Plasmids containing a small *Cla*I/*Bam*HI fragment and which did not cut with *Nde*I (Y80F eliminates a unique *Nde*I site) contained the desired mutations.

Protein Synthesis Inhibition Assay. Enzyme activity was monitored as dose response curves, and relative activities were deduced by comparing 50% inhibitory concentrations (IC_{50}) under standard conditions. RTA was incubated for 5 min at 25 °C with 350 nM *Artemia salinas* ribosomes (purified as described by Kramer *et al.*, 1975), the reaction was stopped by addition of anti-RTA antibodies, and residual ribosome activity was measured as previously described (Ready *et al.*, 1983).

Cytotoxicity Assay. The ability of RTA to kill cells by fluid phase uptake was monitored by [^{35}S]methionine incorporation of remaining viable cells following a 20 h incubation with toxin (Better *et al.*, 1992, 1993). HSB2 cells in log phase were diluted to 10^6 cells/mL in RPMI 1640 media in the absence of methionine, and 0.1 mL was dispensed into each well of a 96 well Costar plate. Toxin dilutions (0.1 mL) were added in triplicate, and the plate was incubated at 37 °C for 20 h. Following a 4 h pulse with [^{35}S]methionine (0.1 mL, 1 μCi/mL), cells were harvested onto Whatman glass fiber filter paper using a Brandel Harvester. Filters were counted in Bray's fluor in an LKB LS5000E liquid scintillation counter. Protein synthesis is expressed as a percentage of control incorporation in the absence of toxin.

Tryptic Digestion of RTA. RTA (1 mg/mL) in 100 mM HEPES of various pH values was incubated at 37 °C with 1% (w/w) trypsin. Aliquots (5 mL) were removed at timed intervals, an equal volume of SDS sample buffer was added, and the samples were boiled for 2 min and placed on ice. When all samples were collected, digestion products were separated by SDS PAGE on 15% gels.

Thermal Denaturation of RTA. RTA R180H (1 mg/mL) was incubated at 40 °C for 5 min in a total volume of 70 μL of 0.1 M HEPES at a variety of pH values. Denatured protein samples were pelleted by centrifugation, and 5 μL supernatant aliquots were analyzed by electrophoresis on 12% polyacrylamide gel.

Inactivation of RTA with Diethyl Pyrocarbonate (DEPC). RTA in 0.1 M sodium phosphate (pH 7.5) was incubated at 25 °C for 1 h with 1 mM DEPC. An equal volume of 0.1 M sodium phosphate (pH 7.5)/10 mM imidazole was added to quench the reaction, and a 20 μL aliquot was removed, diluted appropriately in 20 mM HEPES (pH 7.5), and assayed in the standard protein synthesis inhibition assay.

Crystallization of RTA R180H. RTA R180H failed to yield crystals from the usual high pH conditions (Robertus *et al.*, 1987), but gave large crystals from low pH conditions similar to those described by Weston *et al.* (1994). Crystals were grown by the sitting drop method using micro-bridges (Hampton Research). A 40 μL aliquot of protein [4 mg/mL in 5 mM phosphate (pH 6.5)/150 mM sodium chloride] was added to 20 μL of reservoir solution [0.5 M ammonium sulfate/0.1 M sodium acetate (pH 4.5)] and equilibrated against 200 μL of reservoir solution at 4 °C. Crystals (∼1 × 0.5 × 0.5 mm) grew over a few weeks and belonged to the tetragonal space group $P4_12_12$ ($a = b = 68.8$ Å, $c = 141.2$ Å).

As activity assays were performed at pH 7.6, it seemed useful to obtain crystal data at the same pH. Attempts to grow crystals at higher pH proved fruitless, so crystals grown at pH 4.5 were transferred to 50 μL microdialysis buttons (Cambridge Repetition Engineers) containing 50 μL of 0.1 M MES (pH 6.0)/1.0 M ammonium sulfate ± adenosine monophosphate (AMP) and dialyzed against 20 mL of the same. The solutions were then titrated to pH 7.0, 7.5, or 8.0 with potassium hydroxide and incubated at 4 °C for up to 2 weeks. Crystals titrated to pH 8.0 dissolved within 2 weeks. Crystals titrated to pH 7.0 and 7.5 showed some decay but still diffracted to 2.6 Å and retained essentially the same cell parameters as the untreated crystals.

Diffraction data were collected with a San Diego multiwire area detector system at room temperature (Hamlin, 1985; Howard *et al.*, 1985). Data for the RTA R180H apoenzyme (pH 4.5) were collected to 2.2 Å resolution from a single crystal using Cu Kα radiation. A total of 379 920 observations were reduced to a unique set of 18 873 reflections (*R*

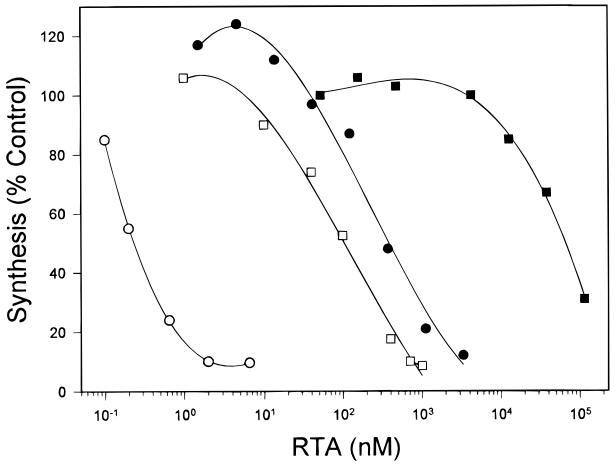

FIGURE 1: Inhibition of protein synthesis against *A. salinas* ribosomes (open symbols) or HSB2 T-cells (solid symbols) with wild-type RTA (circles) and R180H (squares).

merge 7.6%). The data were 99.8% complete to 2.2 Å. The wild-type RTA structure of Weston *et al.* (1994) was used as a starting model for structure determination. Active site residues were omitted from initial map calculations (of the form $2F_o - F_c$) to reduce bias in the fitting of the mutation. Model building was performed using the interactive graphics program FRODO (Jones, 1982) on an Evans and Sutherland PS390 system, and the model was refined by energy minimization and simulated annealing using the program X-PLOR (Brunger *et al.*, 1987). The final model has an *R* factor of 21.4% for reflections from 10 to 2.2 Å and RMS deviation from ideality of 0.013 Å and 2.75° for bond lengths and angles, respectively.

The RTA R180H·AMP data were refined using energy minimization in X-PLOR as above with the RTA R180H apoenzyme structure as a starting model. The model has an *R* factor of 19.75% for data from 10 to 2.8 Å.

RESULTS AND DISCUSSION

Enzyme Activity of RTA R180H. Substitution of Arg 180 with histidine was previously reported to reduce *N*-glycosidase activity by at least 1000-fold against rabbit reticulocyte ribosomes (Frankel *et al.*, 1990). In this study, activity was measured against *Artemia salinas* ribosomes. A dose response assay shows the wild-type RTA has an IC_{50} of 0.2 nM (Figure 1). R180H was consistently observed to be much less toxic than wild-type, with an IC50 of ~100 nM (500-fold higher than wild-type) and requiring near-equimolar amounts of enzyme and substrate to achieve maximal inhibition over the 5 min incubation time of the standard assay. The enzyme does turn over substrate, however, as shown by incubation with lower enzyme concentrations for longer time periods. Activity assays were carried out on at least four different preparations of RTA R180H and yielded essentially the same results in each case.

Inactivation with Diethyl Pyrocarbonate. In order to confirm that the observed activity of R180H was due to a catalytic histidine and not simply due to wild-type contamination, RTA R180H was treated with diethyl pyrocarbonate (DEPC), a histidine specific reagent. Figure 2 shows that R180H activity is readily inhibited by this reagent, whereas wild-type RTA activity is unaffected by the treatment.

AMP is a substrate analog for RTA which binds in the active site and can be depurinated by the enzyme (Weston

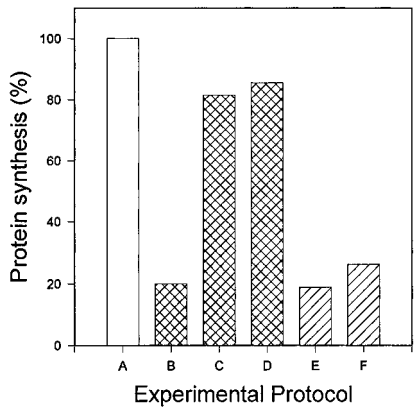

FIGURE 2: Inhibition of R180H activity by treatment with diethyl pyrocarbonate as described under Experimental Procedures. (A) Untreated ribosomes are shown as open bar. Ribosomes attacked by R180H are cross hatched: (B) untreated R180H; (C) R180H preincubated with DEPC; (D) R180H preincubated with DEPC in the presence of 10 mM AMP. Data for wild-type RTA are shown with diagonal lines: (E) untreated wild-type RTA; (F) RTA preincubated with DEPC.

et al., 1994). Therefore, it might be expected that AMP could block the active site of R180H and protect it against inactivation by DEPC. A 5 mM nucleotide concentration is sufficient to observe binding in wild-type RTA (Monzingo & Robertus, 1992; Weston *et al.*, 1994); however, preincubation of R180H with 10 mM AMP provided no protection against DEPC inactivation (Figure 2). This suggests that the R180H substitution results in reduced substrate binding or in a conformational change which exposes a previously inaccessible residue.

Cytotoxicity of RTA R180H. Ricin is extremely cytotoxic to many eukaryotic cells, but RTA, which lacks the cell surface binding B-chain, is much less cytotoxic. Cytotoxicity can still be readily measured against HSB2 T-cells, which have both receptor mediated and fluid phase uptake systems. RTA has an IC_{50} of 300 nM (compared with 10 pM for ricin holotoxin) for cytotoxicity against these cells (Figure 1). Again, activity of the R180H mutant enzyme is drastically reduced, having an IC_{50} of ~70 mM (230-fold less active than wild-type).

Modeling of the R180H and R180Q Substitutions. To help rationalize observations about Arg 180 mutations, the RTA·FMP complex model (Monzingo & Robertus, 1992) was altered to substitute Gln and His at position 180. The models were energy minimized using X-PLOR and revealed that NE2 of the introduced histidine is too far away from N3 of the substrate purine ring (4.9 Å) to hydrogen bond or directly protonate it. The loss of this interaction should reduce both substrate binding and catalysis. Introduction of a water molecule between NE2 of His 180 and the substrate N3 allows a compensating interaction to be made, as shown in Figure 3. The bound water helps to orient the substrate, and the His can indirectly protonate the purine leaving group through the intervening water molecule, mimicking the role of the wild-type Arg 180.

Substitution of Arg 180 with glutamine also inserts a side chain at position 180 which is too short to directly hydrogen bond to N3 of the substrate, but which, like the model of RTA R180H, could also make interactions via a bridging water molecule. The observed kinetic parameters of RTA R180Q, with greatly decreased k_{cat} but unchanged K_m (Ready *et al.*, 1991), are consistent with this model. The ~1000-

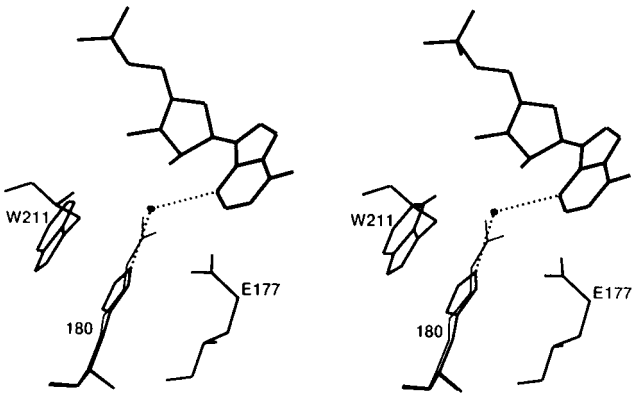

FIGURE 3: Model complex between FMP and RTA mutant protein. A stereoview is shown of an energy minimized model of the putative R180H·FMP complex with a water molecule bridging between NE2 of His 180 and N3 of the formycin ring. Broken lines represent putative hydrogen bonds. FMP is drawn with bold bonds. The position of Arg 180 from the wild-type complex is shown in thin bonds.

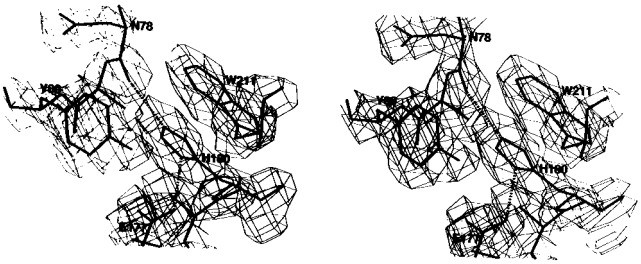

FIGURE 4: Stereoview of the active site of R180H apoenzyme with $2F_o - F_c$ electron density contoured at the 1σ level.

fold decrease in k_{cat} presumably results from the inability of Gln to donate a proton to the leaving group and hence facilitate catalysis. Substitution with histidine might be expected to result in a protein with higher activity than RTA R180Q because the side chain imidazole could function as a proton donor through the intervening water molecule. The observed activity of RTA R180H is, however, lower than that of RTA R180Q, suggesting that the energy minimized model does not accurately represent the true conformation of this substitution.

Structure of RTA R180H. R180H at concentrations of 2−3 mg/mL precipitates at basic pH, but is soluble to >7 mg/mL at acid pH, and attempts to obtain crystals at high pH proved fruitless. However, crystals were readily obtained at pH 4.5 in similar conditions to those used by Weston *et al*. (1994) to obtain wild-type. These R180H crystals were isomorphous with the wild-type and 2.2 Å data collected as described in Experimental Procedures. The structure of Weston *et al.* was used as a starting model for structure determination.

The principal differences between wild-type and the R180H protein all occur in the active site, which is shown in Figure 4. Tyrosine 80 rotates approximately 60° into a position which completely blocks the active site. The tyrosyl hydroxyl moiety moves 5.6 Å to form a hydrogen bond with OE1 of glutamate 177 (2.9 Å), another critical active site residue. The hydroxyl also hydrogen bonds to water 407 (2.6 Å) which is in turn involved in a network of hydrogen bonds with water 352 and the main chain carbonyl group of residue 208. The imidazole ring of His 180 is clearly defined in the electron density map and stacks almost parallel with Trp 211, the rings being separated by 3.5 Å. The motion of

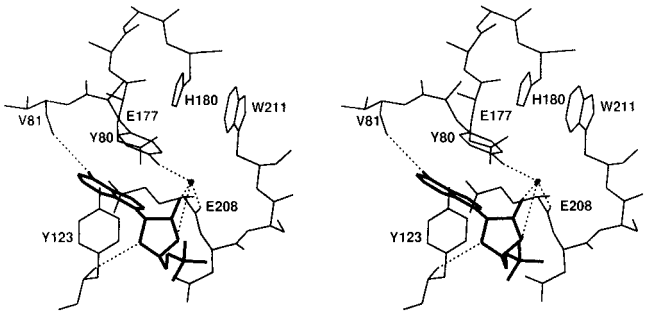

FIGURE 5: Stereoview of the active site of R180H with AMP bound in the active site. Potential hydrogen bonds with the ligand are shown as dashed lines, while the ligand is drawn with bold bonds.

Tyr 80 places it into a position to form favorable aromatic interactions with the imidazole of His 180. Tyrosine 123 has moved ~0.7 Å to retain interactions with the aromatic ring of Tyr 80 and to form a hydrogen bond with OE1 of glutamate 177. The four ring structures form a complex reminiscent of a hydrophobic core, with parallel stacking and edge on face interactions (Singh & Thornton, 1985; Burley & Petsko, 1985).

The His 180 imidazole donates a hydrogen bond to the main chain carbonyl oxygen of Asn 78 (2.7 Å). Also, the ND1 of His 180 appears to donate a bond to OE2 of Glu 177 (2.8 Å), so it is likely that His 180 is present in the fully protonated form in this crystal.

Enzyme activity assays are performed at pH 7.6 where an imidazole ring of normal pK_a would be mostly deprotonated and therefore unable to donate a proton to the leaving group. To examine this, R180H crystals were titrated to pH 7.5 and equilibrated at 4 °C for 2 weeks prior to data collection. The X-ray structure obtained from these crystals was identical to that at pH 4.5. This is consistent with the notion that the histidine remains mostly protonated at pH 7.5, that no disruptive change in charge at the active site has occurred, and that the enzyme at pH 7.5 is in a state in which it could potentially function as a catalytic acid.

Tyr 80 in wild-type RTA partially blocks the adenine binding, but moves to accommodate AMP or FMP during cocrystallization experiments (Monzingo & Robertus, 1992; Weston *et al.*, 1994). Tyr 80 in R180H is in a more extreme position blocking the active site cleft. To test if the residue could be displaced, both cocrystallization of R180H with 25 mM AMP and soaking of preformed crystals with 500 mM AMP were attempted. Both failed to yield a structure with bound AMP or bound cleavage product, adenine, providing evidence for the reduced binding affinity of this mutant for substrate analogs.

Structure of RTA R180H with Bound AMP. Cocrystallization of R180H with 250 mM AMP did produce a bound complex. Difference density maps revealed that AMP was indeed bound in the active site area. Surprisingly, the structure of the protein in the complex is essentially unchanged from that of the apoenzyme (Figure 5). Compared with the wild-type enzyme, the bound purine makes few hydrogen bonds (N6 donates to the main chain carbonyl group of residue 81) and the ribose moiety forms hydrogen bonds to a water molecule (via O2′ and O3′) and to the main chain amino group of residue 123. The phosphate moiety is clearly defined, but appears to form no direct interactions with the protein.

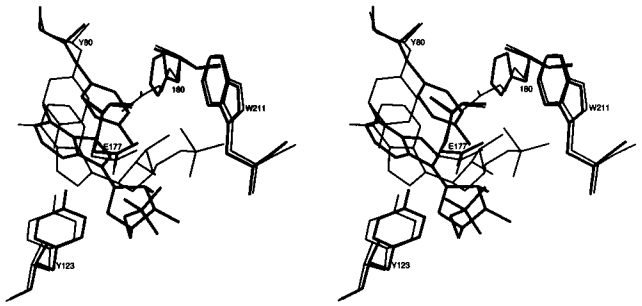

FIGURE 6: Stereoview of the superposition of the observed R180H·AMP and RTA·FMP complexes. The bonds representing the active site residues and bound nucleotide of the R180H·AMP complex are shown in heavy bonds, while the RTA·FMP complex is shown in light bonds.

Tyr 80 is not displaced when AMP binds to reveal a wild-type adenine recognition cleft, but remains in a position to completely block access to His 180. That is, in the configuration of the crystalline complex neither His 180, nor any intervening water molecule, can donate a hydrogen bond to N3 of the potential leaving group. As shown in Figure 6, the adenine ring is rotated roughly 70° compared with the formycin ring of RTA·FMP or the adenine ring of RTA·ApG (Monzingo & Robertus, 1992). Such a large disruption of the catalytic machinery and substrate orientation in the R180H·AMP complex would seem to be more devastating than the observed 500-fold loss of activity for this mutant. When RTA binds rRNA as a substrate, many additional interactions are made outside the adenine recognition cleft (Monzingo & Robertus, 1992). It may be that when R180H attacks ribosomes, additional binding forces are brought to bear which force Tyr 80 to move as seen in wild-type, forming a better pocket and allowing partial protonation of N3 by His 180 through the intervening water molecule. The complex we observe with a mononucleotide analog appears to be abortive and does not represent the productive binding for rRNA. Even so, it seems likely that the R180H enzyme will have reduced affinity for substrate due to its disrupted binding site, and will also have reduced catalytic rate due to its loss of an optimum proton donor for N3.

RTA Double Mutant Y80F/R180H. In the wild-type RTA structure, the hydroxyl moiety of Tyr 80 forms a hydrogen bond with the main chain carbonyl oxygen of Gly 121. This bond is broken when substrate displaces the tyrosyl side chain to form aromatic stacking interactions with the bound adenine ring (Monzingo & Robertus, 1992). The carbonyl oxygen of Gly 121 hydrogen bonds to N6 of adenine. Removal of the hydroxyl group from Tyr 80 to form Phe (Y80F) results in a 20-fold increase in K_m for ribosomes and a 10-fold decrease in k_{cat} in the wild-type enzyme (Ready *et al.*, 1991).

In contrast to the wild-type, R180H structure shows that the hydroxyl group of Tyr 80 forms a charged hydrogen bond with Glu-177, an interaction which is perhaps more difficult to break in order to permit substrate binding. Furthermore, the tyrosyl ring forms favorable aromatic interactions with His 180 and Tyr 123. These additional interactions probably stabilize the unliganded form of R180H and hence reduce binding. To examine the role of the Tyr 80 bond on the R180H protein, a double mutant was constructed. Unfortunately, introduction of the Y80F substitution into an R180H background resulted in a protein which was expressed at such a low level it could not be purified for analysis.

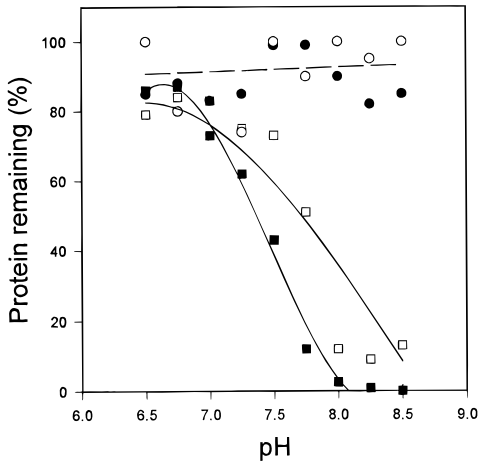

FIGURE 7: Effect of pH on thermostability (solid symbols) and proteolytic sensitivity (open symbols) of wild-type RTA (circles) and R180H (squares).

Thermal Stability of R180H. R180H remains soluble at 1 mg/mL at 37 °C for more than 1 h, but precipitates in a pH dependent manner at 40 °C over a few minutes. Figure 7 shows that, at varying pH values, R180H remains soluble after a 5 min incubation at mildly acid or neutral values, but precipitates as the pH is increased such that at pH 8.5 no soluble protein remains. Wild-type RTA remains soluble at all the pH values tested over the 5 min incubation period.

Stability of RTA R180H to Proteolysis. A second measure of R180H stability is to monitor its sensitivity to proteolysis by trypsin (Figure 7). The activity of trypsin varies ~3-fold over the pH range 6.5−8.5, but is relatively constant between pH 7 and 8.5 (Spomer & Wooton, 1971). Both wild-type and RTA R180H show increasing sensitivity to proteolytic cleavage by trypsin as the pH is increased. However, enhanced sensitivity of R180H is much more pronounced. After a 20 min incubation at 37 °C between pH 7.5 and 8.5, more than 90% of the R180H protein is digested (Figure 7). Under identical conditions wild-type RTA remains essentially intact.

The results of both thermal and proteolytic stability experiments show (i) that R180H has decreased stability compared to wild-type RTA and (ii) that this instability is pH dependent. Thermal denaturation has an apparent pK_a ~7.5 while proteolysis has a pK_a ~7.8. The most likely explanation of these results is that the protonation state of His 180 affects the global stability of the protein. That is, at lower pH, where His 180 is protonated, there is charge balance in the active site and the protein approaches the stability of the wild-type protein. Deprotonation of His 180 leaves a lone negative charge in the active site and results in reduced stability. Other substitutions which alter the active site charge balance, such as RTA R180Q, also greatly reduce stability (Ready *et al.*, 1991). RTA E177A is produced in higher yield and is presumably more stable in vivo, but in its case another acidic residue rotates into the active site to replace the deleted side chain (Kim *et al.*, 1992). If this analysis is correct, it suggests the pK_a for His 80 is ~7.7 and that in the standard assay >50% of the bulk protein is in the protonated form.

Conclusions. Substitution of Arg 180 of RTA with His causes a dramatic decrease in antiribosomal activity and cytotoxicity. Loss of activity is due to a rearrangement of the active site such that Tyr 80 forms a charged hydrogen

bond with Glu 177 and sterically blocks access to His 180. This rearrangement forms a hydrophobic pocket reminiscent of a hydrophobic protein core with favorable interactions among four aromatic side chains. The global stability of the protein is dependent on the protonation state of the histidine. At low pH where the histidine is protonated, the substituted protein approaches the stability of the wild-type protein. At higher pH values, deprotonation results in a charge imbalance in the active site and greatly reduced stability.

The aromatic pocket formed by the R180H substitution is very stable and greatly reduces or even precludes productive binding of small substrate analogs; even 250 mM AMP is insufficient to break the Tyr 80 to Glu 177 bond and allow formation of a productive complex. Larger substrates may be able to assume a more normal binding mode, with the target adenine bound as modeled in Figure 3. An interesting feature of the observed AMP complex is the fact that although AMP does not bind in the same conformation as that of the wild-type·FMP complex, it still binds in the active site and not in any other of the nucleotide binding sites.

REFERENCES

Better, M., Bernhard, S. L., Lei, S.-P., Fishwild, D. M., & Carroll, S. F. (1992) *J. Biol. Chem.* 267, 16712−16718.

Better, M., Bernhard, S. L., Lei, S.-P., Fishwild, D. M., Lane, J. A., Carroll, S. F., & Horwitz, A. H. (1993) *Proc. Natl. Acad. Sci. U.S.A. 90*, 457−461.

Brunger, A., Kuriyan, J., & Karplus, M. (1987) *Science 235*, 458−460.

Burley, S. K., & Petsko, G. A. (1985) *Science 229*, 23.

Endo, Y., & Tsurugi, K. (1987) *J. Biol. Chem. 262*, 8128−8130.

Frankel, A., Welsh, P., Richardson, J., & Robertus, J. D. (1990) *Mol. Cell Biol. 10*, 6257−6263.

Hamlin, R. (1985) *Methods Enzymol. 114*, 416−452.

Howard, A. J., Nielson, C., & Xuong, N. H. (1985) *Methods Enzymol 114*, 453−472.

Jones, T. A. (1982) FRODO: A graphics fitting program for macromolecules. In: *Computational Crystallography* (Sayre, D., Ed.) pp 303-317 Oxford University Press, Oxford.

Katzin, B., Collins, E. J., & Robertus, J. D. (1991) *Proteins: Struct., Funct., Genet. 10*, 251−259.

Kim, Y., & Robertus, J. D. (1992) *Protein Eng. 5*, 775−779.

Kramer, G. A., Pinphanicharan, P., Konecki, D., & Hardesty, B. A. (1975) *Eur. J. Biochem. 53*, 471−480.

Mol, C. D., Arvai, A. R., Slupphaug, G., Kavil, B., Alseth, I., Krokan, H. E., & Tainer, J. A. (1995) *Cell 80*, 869−878.

Montfort, W., Villafranca, J. E., Monzingo, A. F., Ernst, S. R., Katzin, B., Rutenber, E., Xuong, N. H., Hamlin, R., & Robertus, J. D. (1987) *J. Biol. Chem. 262*, 5398−5403.

Monzingo, A. F., & Robertus, J. D. (1992) *J. Mol. Biol. 227*, 1136−1145.

Olnes, S., & Pihls, A. (1992) In *The Molecular Action of Toxins and Viruses* (Cohen, P., & Van Heynigen, S. Eds.) pp 52−105, Elsevier Biomedical Press, New York.

Ready, M. P., Bird, S., Rothe, G., & Robertus, J. D. (1983) *Biochim. Biophys. Acta 740*, 19−28.

Ready, M. P., Kim, Y., & Robertus, J. D. (1991) *Proteins: Struct., Funct., Genet. 10*, 270−278.

Ren, J., Wang, Y., Dong, Y., & Stuart, D. I. (1994) *Structure 2*, 7−16.

Robertus, J. D., Piatak, M., Ferris, R., & Houston, L. L. (1987) *J. Biol. Chem. 262*, 19−21.

Rutenber, E., Katzin, B., Collins, E. J., Mlsna, D., Ernst, S. R., Ready, M. P., & Robertus, J. D. (1991) *Proteins: Struct., Funct., Genet. 10*, 240−250.

Savva, R., McAuley-Hecht, K., Brown, T., & Pearl, L. (1995) *Nature 373*, 487−493.

Schlossman, D., Withers, D., Welsh, P., Alexander, A., Robertus, J. D., & Frankel, A. (1989) *Mol. Cell Biol. 9*, 5012−5021.

Singh, J., & Thornton, J. M. (1985) *FEBS Lett. 191*, 1.

Spomer, W. E., & Wooton, J. F. (1971) *Biochim. Biophys. Acta 235*, 164−171.

Weston, S. A., Tucker, A. D., Thatcher, D. R., Derbyshire, D. J., & Pauptit, R. A. (1994) *J. Mol. Biol. 244*, 410−422.

BI960880N